

Nickel–Thiolate Complex Catalyst Assembled in One Step in Water for Solar H₂ Production

Wei Zhang,[†] Jindui Hong,[†] Jianwei Zheng,[‡] Zhiyan Huang,[§] Jianrong (Steve) Zhou,[§] and Rong Xu^{*,†}

[†]School of Chemical & Biomedical Engineering, Nanyang Technological University, 62, Nanyang Drive, Singapore 637459, Singapore

[‡]Institute of High Performance Computing, Agency for Science, Technology and Research, 1 Fusionopolis Way, #16-16 Connexis, 138632, Singapore

[§]School of Physical and Mathematical Sciences, Nanyang Technological University, Singapore 637371, Singapore

S Supporting Information

ABSTRACT: We report the use of a simple complex assembled from Ni(II) salt and 2-mercaptoethanol in one step in water as the efficient catalyst in a molecular hydrogen system which can be sensitized by a low-cost xanthene dye, Erythrosin B. An excellent quantum efficiency of 24.5% is attained at 460 nm. This simple system is expected to contribute toward the development of economical and environmentally benign solar hydrogen production systems.

Photocatalytic hydrogen production from water represents an important process in sustainable solar energy conversion for the future. This process can be realized by using the molecular hydrogen system which can provide a homogeneous reaction environment toward optimal availability of active catalytic sites for solar hydrogen production.¹ Such a system typically comprises a metal complex photosensitizer (PS), e.g., Ru(bpy)₃²⁺, for solar light harvesting and a metal-based catalyst, such as metallic colloidal Pt or Pt-complexes for receiving the electrons from the excited PS directly or via an electron relay. Despite the promising findings so far, the frequent use of precious metals and/or complicated structures associated with the photosensitizers or catalysts limits their potential wide applications.

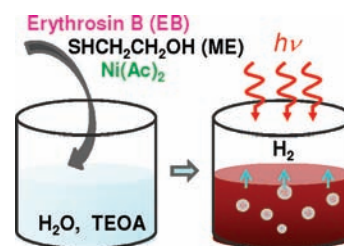
Back in 1975, Balzani et al. conceptually showed that transition metal complexes are in principle suitable catalysts for the photodissociation of water.² A few promising examples of using transition metal complex based catalysts have been reported so far, including metalloporphyrin complexes,^{3a,b} [Co^{III}(dmgH)₂pyCl],^{3c,d} and the bioinspired nickel phosphine type complexes.^{3e,f} Nonetheless, these molecular complexes have relatively complicated structures and may not be easily synthesized. It is highly desirable to use a simple process toward the preparation of low-cost molecular systems for photocatalytic hydrogen production potentially at a large scale.

In our recent study, inorganic NiS nanoparticles were found capable of replacing the Pt cocatalyst in the well-known Pt/CdS semiconductor photocatalysts while exhibiting an excellent quantum efficiency of 51% under visible light.⁴ This phenomenon inspired us to employ the low-cost transition metal–sulfur complexes as the catalysts in the molecular hydrogen systems. Herein, we report the use of a simple complex assembled from a Ni(II) salt and 2-mercaptoethanol in

one step in water as the efficient catalyst in a molecular hydrogen system which can be sensitized by low-cost xanthene dyes. This simple system is expected to contribute toward the development of economical and environmentally benign solar hydrogen production systems.

The molecular hydrogen system consisting of all earth-abundant elements was assembled by mixing nickel(II) acetate (3 mM) and 2-mercaptoethanol (ME) (30 mM) to form the catalyst complex in the aqueous solution containing triethanolamine (TEOA, 15 vol%) as the sacrificial reagent, followed by adding Erythrosin B (EB, 2.25 mM) as the PS (Scheme 1). The

Scheme 1. A Simple Process to Assemble the EB–Ni–ME Molecular System from Earth-Abundant Elements



resultant system is denoted as EB–Ni–ME. Toxic solvents like acetonitrile or toluene commonly used in other molecular hydrogen systems to better dissolve the metal complexes are not required in our system. In the aqueous solution, Ni²⁺ ions and the ME ligands upon mixing and dissolving readily form the dark brown colored complex. The majority of the Ni–ME complex appears to be homogeneous in the solution although a very small portion of the precipitates can be separated by high speed centrifugation.

Figure 1A shows the time course of hydrogen evolution over the EB–Ni–ME system. The experimental parameters including the concentrations of EB, Ni²⁺ ions, and TEOA; Ni/S ratio; and the pH have been optimized. It is found that the EB–Ni–ME system can efficiently generate 9.5 mmol of hydrogen gas in the first 12 h of irradiation of visible light ($\lambda > 420$ nm) corresponding to a high average production rate of 792 μ mol/h. A moderate quantum efficiency of 12% is obtained

Received: September 10, 2011

Published: December 1, 2011

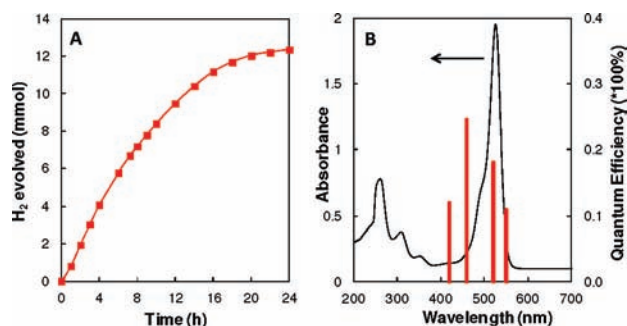


Figure 1. (A) Time course of photocatalytic hydrogen evolution over EB–Ni–ME system (light source: 300 W Xe lamp, $\lambda > 420$ nm, 100 mL solution, pH = 8.5). (B) UV–vis absorption spectrum of EB and the quantum efficiencies of hydrogen evolution under photons with different wavelengths over the EB–Ni–ME system.

at 420 nm with a band-pass filter. Our system exhibits relatively good stability in a single run compared to other molecular systems reported,^{1g,3c,d} as the major slowdown happens only after 16 h which is due to degradation of EB (to be discussed shortly). The total amount of H₂ produced from this system is about 12.3 mmol in 24 h. Even under photons of longer than 500 nm wavelength, our system can still efficiently generate 8.2 mmol of hydrogen in 24 h (Figure S1). The measured quantum efficiencies under photons at different wavelengths are shown Figure 1B. The highest quantum efficiency of 24.5% is obtained at 460 nm, which is shorter than the wavelength of the highest absorption of EB at 524 nm in the visible light range. At 550 nm, the quantum efficiency is still as high as 11.0%. To the best of our knowledge, these values are among the highest reported for the molecular hydrogen systems in the visible light range. To confirm that hydrogen is generated from water instead of other components, the photoreaction in a D₂O solution while keeping other conditions identical was conducted based on similar procedures reported in our previous study.⁴ The same amount of D₂ gas was obtained in 24 h, indicating that the only hydrogen source in the produced hydrogen gas is water.

Several reports can be found from the literature dealing with the structures of the complexes between Ni(II) and primary thiolates.⁵ De Brabander et al. proposed a linear “core + link” polymeric complex between Ni(II) and ME in dilute aqueous solutions based on a titration method.^{5a} On the other hand, Gould and Harding precipitated the crystal from an alkaline solution of concentrated Ni(II) and ME. Their X-ray diffraction data indicated a cyclic hexameric complex with six Ni(II) ions forming a planar ring and the Ni(II) centers bridged by twelve ME thiolates.^{5b} A few other groups also proposed the hexagonal structure between Ni(II) and ME or other thiolate.^{5c–e} In order to determine the structure of the Ni–ME complex formed under our conditions and to investigate the influence of TEOA, UV–vis absorption and electrospray ionization-mass spectrometry (ESI-MS) analyses were carried out. Figure S2 shows the UV–vis absorption spectra of the Ni–ME complex in DI water (pH = 8.5, adjusted by NaOH) and an aqueous solution containing TEOA (pH = 8.5). In both cases, four characteristic charge transfer bands can be observed at nearly the same wavelength of 258, 330, 408, and 525 nm, indicating that TEOA does not affect coordination between Ni(II) and ME thiolate. Nevertheless, the absorption intensities of Ni–ME in TEOA solution were slightly lower than those in DI water. We further diluted both solutions and compared their absorption intensities as shown in Figure S3 and Table S1. The

concentration of the Ni–ME complex in TEOA solution was estimated to be around 90% of that in DI water when [Ni²⁺] was in the range of 0.3–1.0 mM (Table S2). Positive ion ESI-MS analysis was further carried out to investigate the structure of the Ni–ME complex formed in the solutions. It was found that the Ni–ME complex formed in DI water has a formula of [Ni(SCH₂CH₂OH)₂]₆ (Figure S4A and Table S3). The MS spectrum of nickel acetate in TEOA solution shows a dominant peak at $m/z = 823$ (Figure S4B) which should correspond to the colorless tetramer formed between Ni(II) and TEOA. Finally, the spectrum of Ni–ME in TEOA solution suggests the presence of both Ni–ME ($m/z = 1298$) and tetramer Ni–TEOA ($m/z = 823$) complexes (Figure S4C). In addition, a peak at $m/z = 1448$ was observed, which can be assigned to [Ni(SCH₂CH₂OH)₂]₆ associated with one TEOA ($m/z = 1448 - 1298 = 150$, MW of TEOA = 149). Although the peak of the [Ni(TEOA)]₄ complex ($m/z = 823$) is rather strong compared to those of [Ni(SCH₂CH₂OH)₂]₆ complexes, such results are not reliable for quantitative analysis due to the need to produce charged ions of all complexes and fragmentation of molecular ions under the ESI conditions. As mentioned above based on the UV data, it could be estimated that about 10% of Ni(II) forms a complex with TEOA and 90% of Ni(II) remains in the complex with ME as [Ni(SCH₂CH₂OH)₂]₆. Based on the above results and literatures,⁵ it is proposed that the Ni–ME complex formed in TEOA solution adopts a cyclic structure (Figure S5A), although we could not exclude the existence of a linear structure in equilibrium (Figure S5B). TEOA can also coordinate with a small fraction of Ni(II) but does not affect the coordination in the majority of [Ni(SCH₂CH₂OH)₂]₆.

EB has four iodide substitutions on its xanthene ring. Similar to other heavy halogen-substituted xanthene dyes, the C–I bond in EB could be cleaved quickly through reductive quenching leading to its photodegradation and deterioration of activity.⁶ However, in our EB–Ni–ME system, EB is relatively stable. As shown in Figure S6A, the intensity of the absorption does not change significantly even at 8 h of irradiation. The peak position blue shifts from 524 to 502 nm, which is associated with the partial loss of iodide of EB. At 24 h, the absorption peak has become much weaker and the peak position further shifts to 488 nm corresponding to mainly the absorption of Fluorescein after total dehalogenation of EB. The ESI-MS analysis of the reaction mixture provided the consistent results about the progressive loss of iodide groups from EB during the light irradiation (Table S4). The absorption ability of the Ni–ME complex in the range of 460 to 600 nm overlaps with that of EB (Figure S6B) indicating that Ni–ME can quench the excited EB efficiently.

Our Ni–ME complex has been shown to be an efficient electrocatalyst for the reduction of protons to molecular hydrogen based on the cyclic voltammetric study. As shown in Figure 2A, similar to other Ni-complexes,^{3c,f} the Ni–ME complex displays an irreversible reduction wave at around -0.69 V (vs SCE) which should be associated with the reduction of Ni(II) to the reactive Ni(I) center. After adding acetic acid (HAc) to the solution, the current was greatly enhanced and the electrocatalytic proton reduction potential was shifted slightly more negative to -0.73 V. Similar observations were reported by other groups for transition metal complexes of nickel and iron.^{3a,e,f} The oxidation and reduction potentials of EB obtained by the cyclic voltammetric studies are $+0.88$ and -1.05 V, respectively. The reduction potential of TEOA was measured to be -0.55 V. By comparing

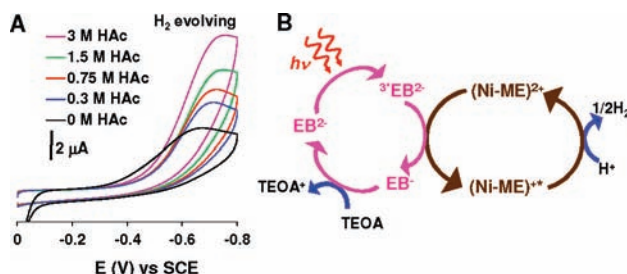


Figure 2. (A) Cyclic voltammogram of Ni–ME complex formed between nickel(II) acetate (30 mM) and ME (60 mM) in water; a glassy carbon working electrode; scan rate at 100 mV/s. (B) Proposed reaction scheme of the photocatalytic hydrogen production over the EB–Ni–ME molecular system.

these redox potentials, it is suggested that an oxidative quenching pathway of the photosensitized EB by TEOA is supported. Based on the above results, the reaction scheme of the EB–Ni–ME molecular system for photocatalytic hydrogen production in TEOA sacrificial solution is proposed in Figure 2B. EB^{2-} (a divalent anion when dissolved in water) absorbs visible light efficiently to form the excited triplet state, $^3\text{EB}^{2-}$. The excited electron in $^3\text{EB}^{2-}$ is transferred to the Ni–ME complex, leaving the oxidized EB^- . Following the photosensitization and electron injection to Ni–ME, a reactive reduced Ni(I) center is formed which plays a critical role in electron transfer to a proton for hydrogen production. Further, the presence of the basic sulfur groups surrounding the Ni center could facilitate the formation of Ni-hydride for subsequent electrochemical desorption leading to hydrogen evolution.^{4,7} The oxidized EB^- is reduced back to EB^{2-} by TEOA as the sacrificial electron donor.

Besides EB, other xanthene dyes have also been investigated and their molecular structures are shown in Figure S7. Figure

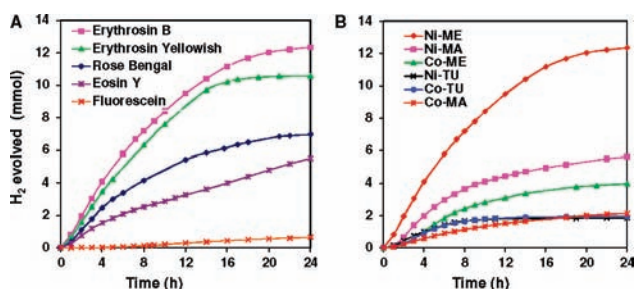


Figure 3. Time course of hydrogen evolution using (A) different xanthene dyes as the PSs and Ni–ME as the catalyst and (B) EB as the PS, and Ni^{2+} and Co^{2+} complexed with different ligands, ME, MA (mercaptoacetic acid) and TU (thiourea) as the catalysts. Light source: 300 W Xe lamp, $\lambda > 420$ nm, 100 mL solution, pH = 8.5.

3A indicates that, among these dyes with different halogen substitutions to the xanthene ring, EB outperforms the others in activity. The halogen-free Fluorescein exhibits a much lower hydrogen evolution rate compared to other xanthene dyes examined. Different halogenation substitutions affect the ground and excited states of xanthene dyes resulting in harvesting photons with different wavelengths and generating electrons of different potentials. On the other hand, the heavy iodine and bromine atoms can facilitate the formation of long-lived triplet states of xanthene dyes from their excited singlet states through intersystem crossing.⁸ Based on the spin

conservation rule (Wigner Rule), the PS in its long-lived excited triplet state can sensitize the catalyst toward forming its own long-lived excited triplet state and, thus, enhance the photocatalytic activity. The optimum performance achieved with the use of EB as the PS suggests the balance of these two aspects in EB. Due to dehalogenation of EB during reaction (verified through UV–vis and ESI–MS analysis as discussed above), the loss of iodide groups from EB eventually resulted in a lower H_2 production activity as the irradiation time was increased. Compared with EB, Fluorescein (FL) is a relatively more photostable dye, although the activity of the FL–Ni–ME system was much lower (Figure 3A). Hence, we conducted a long-term photoreaction using the FL–Ni–ME system to investigate the stability of the Ni–ME catalyst. As shown in Figure S8, after 4.5 days of continuous reaction, no significant decrease in H_2 production activity was observed, indicating that the Ni–ME complex catalyst is stable.

Figure 3B shows the hydrogen evolution over the molecular systems containing EB as the PS, Ni^{2+} , or Co^{2+} complexed with different sulfur-containing small ligands as the catalysts. Overall, complexes of Ni^{2+} exhibit better activities than those of Co^{2+} . Typically, Ni–ME is about three times higher in activity than Co–ME. Among the nickel complexes, ME is the better capping agent than mercaptoacetic acid (MA) and thiourea (TU). ME is widely used in the synthesis of water-soluble ZnS nanoparticles for its excellent capping ability,⁹ while an excess amount of MA can easily precipitate Ni^{2+} in aqueous solution. Within all the combinations investigated, Ni^{2+} capped with ME homogeneously in solution is shown to be an efficient catalyst for generating hydrogen.

To better understand the reaction mechanism and the activity difference among the Ni complexes, we performed ab initio calculations by using the hybrid B3LYP functional together with an LanL2dz basis set, in conjunction with a polarizable continuum model of solvation (PCM),^{10a,b} as implemented in the Gaussian 09 program package.^{10c} The structures of Ni–ME (both cyclic and linear) and Ni–MA were first optimized in water. Two interesting features can be seen from the simulation. First, the highest occupied molecular orbitals (HOMOs) and the lowest unoccupied molecular orbitals (LUMOs) are located at Ni atoms and the surrounding S atoms in the Ni–ME complex, as shown in Figure 4A. Similar

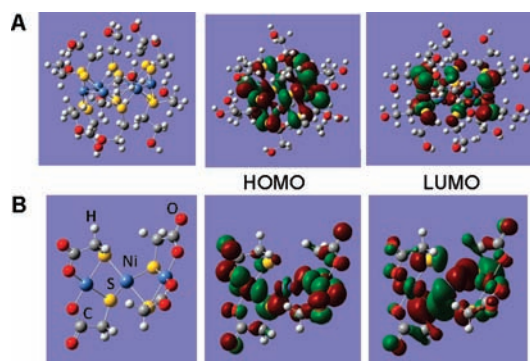


Figure 4. HOMO and LUMO orbitals in (A) cyclic Ni–ME complex and (B) Ni–MA clusters.

results were obtained for the linear Ni–ME cluster as shown in Figure S9. Such results confirm that the Ni and S atoms in the Ni–ME complex are important. However, the HOMOs and LUMOs in the Ni–MA complex are located not only at Ni and

S atoms but also at O atoms (Figure 4B), indicating that O atoms in the Ni–MA complex may also play a role.

Second, Mulliken charge analysis shows that Ni atoms in the Ni–ME complex are negatively charged (Table S5), suggesting that the Ni center in Ni–ME has an electron-rich environment favorable for reduction of protons. For comparison, Ni atoms in the Ni–MA complex are positively charged. Furthermore, we simulated EB–Ni–ME and EB–Ni–MA complexes in water respectively. The binding energy of EB with Ni–ME is 0.35 eV stronger than that of EB with Ni–MA, suggesting that the photogenerated electron in EB is more easily transferred to Ni–ME than to Ni–MA. Moreover, as shown in Table S5, the S atoms in EB–Ni–ME are negatively charged while those in EB–Ni–MA are positively charged. Half of the Ni atoms in EB–Ni–ME bear negative charges while all Ni atoms in EB–Ni–MA are positively charged, showing that Ni–ME is superior to Ni–MA as a reduction center for H₂ production. These simulation results support our experimental data.

In conclusion, the simple EB–Ni–ME molecular system assembled from earth-abundant elements in water in one step shows outstanding photocatalytic efficiencies for hydrogen evolution under visible light. It is believed that such findings present a promising opportunity toward the development of low-cost and environmentally benign solar hydrogen production systems to meet the increasing future energy demand.

■ ASSOCIATED CONTENT

Supporting Information

Experimental methods, Figures S1–S9, and Table S1–S5. Complete ref 10c. This material is available free of charge via the Internet at <http://pubs.acs.org>.

■ AUTHOR INFORMATION

Corresponding Author

rxu@ntu.edu.sg

■ ACKNOWLEDGMENTS

This work was supported by AcRF grants: ARC25/08 from Ministry of Education, Singapore. The authors thank X. Wang for the contribution in cyclic voltammetry studies.

■ REFERENCES

- (1) (a) Du, P. W.; Schneider, J.; Jarosz, P.; Eisenberg, R. *J. Am. Chem. Soc.* **2006**, *128*, 7726–7727. (b) Elvington, M.; Brown, J.; Arachchige, S. M.; Brewer, K. J. *J. Am. Chem. Soc.* **2007**, *129*, 10644–10645. (c) Gartner, F.; Sundararaju, B.; Surkus, A. E.; Boddien, A.; Loges, B.; Junge, H.; Dixneuf, P. H.; Beller, M. *Angew. Chem., Int. Ed.* **2009**, *48*, 9962–9965. (d) Goldsmith, J. I.; Hudson, W. R.; Lowry, M. S.; Anderson, T. H.; Bernhard, S. *J. Am. Chem. Soc.* **2005**, *127*, 7502–7510. (e) Ozawa, H.; Haga, M. A.; Sakai, K. *J. Am. Chem. Soc.* **2006**, *128*, 4926–4927. (f) Rau, S.; Schafer, B.; Gleich, D.; Anders, E.; Rudolph, M.; Friedrich, M.; Gorus, H.; Henry, W.; Vos, J. G. *Angew. Chem., Int. Ed.* **2006**, *45*, 6215–6218. (g) Tinker, L. L.; McDaniel, N. D.; Curtin, P. N.; Smith, C. K.; Ireland, M. J.; Bernhard, S. *Chem.—Eur. J.* **2007**, *13*, 8726–8732. (h) Zhang, X. J.; Jin, Z. L.; Li, Y. X.; Li, S. B.; Lu, G. X. *J. Phys. Chem. C* **2009**, *113*, 2630–2635. (i) Du, P.; Schneider, J.; Fan, L.; Zhao, W.; Patel, U.; Castellano, F. N.; Eisenberg, R. *J. Am. Chem. Soc.* **2008**, *130*, 5056–5058. (j) Sakai, K.; Ozawa, H. *Coord. Chem. Rev.* **2007**, *251*, 2753–2766. (k) Tinker, L. L.; McDaniel, N. D.; Bernhard, S. *J. Mater. Chem.* **2009**, *19*, 3328–3337.
- (2) Balzani, V.; Moggi, L.; Manfrin, M. F.; Bolletta, F.; Gleria, M. *Science* **1975**, *189*, 852–856.
- (3) (a) Kluwer, A. M.; Kapre, R.; Hartl, F.; Lutz, M.; Spek, A. L.; Brouwer, A. M.; van Leeuwen, P.; Reek, J. N. H. *Proc. Natl. Acad. Sci.*

- U.S.A. **2009**, *106*, 10460–10465. (b) Zhang, P.; Wang, M.; Li, C. X.; Li, X. Q.; Dong, J. F.; Sun, L. C. *Chem. Commun.* **2010**, *46*, 8806–8808. (c) Lazarides, T.; McCormick, T.; Du, P. W.; Luo, G. G.; Lindley, B.; Eisenberg, R. *J. Am. Chem. Soc.* **2009**, *131*, 9192–9194. (d) McCormick, T. M.; Calitree, B. D.; Orchard, A.; Kraut, N. D.; Bright, F. V.; Detty, M. R.; Eisenberg, R. *J. Am. Chem. Soc.* **2010**, *132*, 15480–15483. (e) Le Goff, A.; Artero, V.; Jusselme, B.; Tran, P. D.; Guillet, N.; Metaye, R.; Fihri, A.; Palacin, S.; Fontecave, M. *Science* **2009**, *326*, 1384–1387. (f) McLaughlin, M. P.; McCormick, T. M.; Eisenberg, R.; Holland, P. L. *Chem. Commun.* **2011**, *47*, 7989–7991.
- (4) Zhang, W.; Wang, Y. B.; Wang, Z.; Zhong, Z. Y.; Xu, R. *Chem. Commun.* **2010**, *46*, 7631–7633.
- (5) (a) De Brabander, H. F.; Van Poucke, L. C.; Eeckhaut, Z. *Inorg. Chim. Acta* **1972**, *6*, 459–462. (b) Gould, R. O.; Harding, M. M. *J. Chem. Soc. A* **1970**, *6*, 875–881. (c) Jian, F. F.; Jiao, K.; Li, Y.; Zhao, P. S.; Lu, L. D. *Angew. Chem., Int. Ed.* **2003**, *115*, 5900–5902. (d) Wark, T. A.; Stephan, D. W. *Organometallics* **1989**, *8*, 2863–2843. (e) Xiao, H. L.; Jian, F. F.; Zhang, K. J. *Bull. Korean Chem. Soc.* **2009**, *30*, 846–848.
- (6) (a) Shimidzu, T.; Iyoda, T.; Koide, Y. *J. Am. Chem. Soc.* **1985**, *107*, 35–41. (b) Lambert, C. R.; Kochevar, I. E. *Photochem. Photobiol.* **1997**, *66*, 15–25.
- (7) Assuncao, N. A.; Giz, M. J.; Tremiliosi, G.; Gonzalez, E. R. *J. Electrochem. Soc.* **1997**, *144*, 2794–2800.
- (8) Shimidzu, T.; Iyoda, T.; Koide, Y. *J. Am. Chem. Soc.* **1985**, *107*, 35–41.
- (9) Nanda, J.; Sapra, S.; Sarma, D. D.; Chandrasekharan, N.; Hodes, G. *Chem. Mater.* **2000**, *12*, 1018–1024.
- (10) (a) Miertus, S.; Scrocco, E.; Tomasi, J. *Chem. Phys.* **1981**, *55*, 117–129. (b) Pascualahir, J. L.; Silla, E.; Tunon, I. *J. Comput. Chem.* **1994**, *15*, 1127–1138. (c) Frisch, M. J.; et al. *Gaussian 09*, revision A.1; 2009.